A Free Streaming Contact Preserving Scheme for the M_1 Model

C. Berthon[1], J. Dubois[2], B. Dubroca[3], T.-H. Nguyen-Bui[2] and R. Turpault[1,*]

[1] *Université de Nantes, Laboratoire de Mathématiques Jean Leray, 2 Rue de la Houssinière 44322 Nantes Cedex 3, France*

[2] *CEA, CESTA, 33114 Le Barp, France*

[3] *Université Bordeaux I, CELIA, 351 Cours de la libération, 33405 Talence Cedex, France*

Abstract. The present work concerns the numerical approximation of the M_1 model for radiative transfer. The main purpose is to introduce an accurate finite volume method according to the nonlinear system of conservation laws that governs this model. We propose to derive an HLLC method which preserves the stationary contact waves. To supplement this essential property, the method is proved to be robust and to preserve the physical admissible states. Next, a relevant asymptotic preserving correction is proposed in order to obtain a method which is able to deal with all the physical regimes. The relevance of the numerical procedure is exhibited thanks to numerical simulations of physical interest.

AMS subject classifications: 65M06, 85A25.

Key words: Radiative transfer equation, M_1 model, finite volume method, Riemann solver, HLLC scheme, asymptotic preserving scheme.

1 Introduction

The radiative transfer is involved in many applications where its relevant numerical simulation turns out to be essential. However, in several cases where it is coupled with other physics such as hypersonic atmospheric reentry, solving the full radiative transfer equation has a numerical cost beyond the range of the actual computational

ressources and alternative models must be considered. In recent years, several models have been introduced and the present work is devoted to one of them; namely the M_1 model introduced by Dubroca-Feugeas [12].

The M_1 model is known to satisfy several fundamental physical properties (the list is given below). The purpose of this paper is to derive a numerical method which is able to preserve all of these physical properties. Let us emphasize that the numerical experiments of interest involve all the physical regimes and therefore it is essential to have a numerical scheme that can handle all of them.

The system of equations governing the M_1 model comes from the first two moments of the radiative transfer equation (see Dubroca-Feugeas [12] for further details). The considered model reads as follows

$$\partial_t E + \nabla \cdot \mathbf{F} = c\sigma(aT^4 - E), \tag{1.1}$$

$$\partial_t \mathbf{F} + c^2 \nabla \cdot \mathbf{P} = -c\sigma \, \mathbf{F}, \tag{1.2}$$

$$\partial_t(\rho \, C_v T) = -c\sigma(aT^4 - E). \tag{1.3}$$

Here, E denotes the radiative energy and $\mathbf{F} \in \mathbb{R}^2$ the radiative flux vector. The positive constant a is prescribed by physics, while c and σ respectively denote the speed of the light and the opacity. It is to note that the opacity, which will be considered to be constant here for the sake of simplicity, is in general given by non-linear functions of T, E and $\mathbf{F}$ (see [26]). Concerning the radiative pressure $\mathbf{P}$, it is given by

$$\mathbf{P} = \frac{1}{2}\left((1 - \chi(f))\mathbf{I} + (3\chi(f) - 1)\frac{\mathbf{F} \otimes \mathbf{F}}{\|\mathbf{F}\|^2}\right)E, \tag{1.4}$$

with $\quad \chi(f) = \dfrac{3 + 4f^2}{5 + 2\sqrt{4 - 3f^2}}, \tag{1.5}$

where we have introduced the normalized flux vector $\mathbf{f} = \mathbf{F}/cE$, and we have set $f = \|\mathbf{f}\|$.

Let us emphasize that the radiative equations (1.1) and (1.2), issued from the first two moments of the radiative transfer equation, are coupled to the material temperature T governed by Eq. (1.3). We have set ρ the material specific density and C_v the specific heat capacity.

For the sake of simplicity in the notations, we note $U=(E, \mathbf{F}) \in \mathbb{R}^3$ the radiative state vector in the following admissible space

$$\mathcal{A} = \left\{(E, \mathbf{F})^T \in \mathbb{R}^3; \ E \geq 0, \ f \leq 1\right\}.$$

In the following, $W=(E, \mathbf{F}, T)^T$ denotes the state vector defined in the admissible space

$$\Omega = \left\{(E, \mathbf{F}, T)^T \in \mathbb{R}^4; \ (E, \mathbf{F}) \in \mathcal{A}, \ T \geq 0\right\}.$$

There are two main regimes of interest governed by the parameter σ. The first one associated with $\sigma = 0$ coincides with the free streaming regime given by the hyperbolic

system of conservation laws

$$\partial_t E + \nabla \cdot \mathbf{F} = 0, \tag{1.6a}$$

$$\partial_t \mathbf{F} + c^2 \, \nabla \cdot \mathbf{P} = 0, \tag{1.6b}$$

$$\partial_t(\rho \, C_v T) = 0. \tag{1.6c}$$

In computational regions which correspond to such a regime, it is crucial to precisely capture the natural waves of the system. From a numerical point of view, the external waves (rarefactions and shocks) are accurately approximated by any Riemann-type solver. The contact wave, however, requires a specific numerical attention. Therefore, one of our objectives is to derive a numerical scheme that is able to capture it.

On the other hand, whenever σ becomes very large, the system (1.1)-(1.2)-(1.3) degenerates into a nonlinear parabolic equation called the *equilibrium diffusion equation* (see [21, 22]). It is obtained by introducing a rescaling factor ε which can be seen as a Knudsen-like number. Considering long-time behaviors, the rescaled M_1 system becomes

$$\begin{cases} \varepsilon\partial_t E + \nabla \cdot \mathbf{F} = \dfrac{c\sigma}{\varepsilon}(aT^4 - E), \\[2mm] \varepsilon\partial_t \mathbf{F} + c^2\nabla \cdot \mathbf{P} = -\dfrac{c\sigma}{\varepsilon}\mathbf{F}, \\[2mm] \varepsilon\partial_t(\rho C_v T) = -\dfrac{c\sigma}{\varepsilon}(aT^4 - E). \end{cases} \tag{1.7}$$

When ε tends to zero, a Chapman-Enskog expansion of this system allows to recover the so-called equilibrium diffusion equation, which is the asymptotic limit of the radiative transfer equation. This equilibrium diffusion equation is given by

$$\partial_t(\rho C_v T + aT^4) - \nabla \cdot \left(\frac{c}{3\sigma}\nabla T^4\right) = 0. \tag{1.8}$$

In computational regions where σ is very large, we want the numerical scheme to be able to restore a discrete form of the diffusive equation (1.8). This last point is generally very difficult to achieve since the numerical scheme hence has to deal with both an hyperbolic and a parabolic regimes.

The main objective of the present work therefore concerns the derivation of a numerical scheme that admits the following properties:

1. Robustness i.e., conserving the invariance of Ω,
2. Accurate capturing of the waves associated to (1.6) when $\sigma = 0$, in particular to exactly predict the contact waves,
3. Asymptotic preserving i.e., to be consistent with the equilibrium diffusion equation (1.8) whenever σ is large.

Several approaches have been suggested during the last decade to approximate the solutions of the M_1 model. The first one was developed by Dubroca-Feugeas [12]

where an HLL scheme was proposed. This scheme is robust since it preserves the admissible states. Unfortunately such a numerical approach fails to approximate the asymptotic diffusion behavior. To correct such an issue, several techniques were proposed in the literature and the reader is referred to Gosse-Toscani [15], Buet-Cordier [8], Buet-Després [10], Berthon et al. [3–5] for a description of the main numerical methods (see also [1] for another context). In fact, all these techniques are the same strategy. The first step is devoted to the hyperbolic system (1.6), where a standard HLL scheme (see Harten-Lax-Van Leer [17] for the details) is considered. The main benefit of this numerical approximation is an easy preservation of the admissible states for a viscous discretization. Actually, the difference between all the above mentionned works concerns the numerical process used to approximate the source term. For instance in the work of Buet-Cordier [8] (see also [3]), the authors modify the HLL Riemann solver associated with (1.6) to introduce the source term. To access such an issue, a suitable relaxation model is involved to derive a twostep relaxation method. The main comment about this very brief overview concerns the approximation of the transport part of the M_1 model, given by (1.6), which is systematically approximated by the well-known HLL numerical procedure. Indeed, as soon as σ is set equal to zero, all the above cited numerical methods (see also [4,9,11,16]) turn out to coincide with the explicit or implicit HLL scheme for (1.6). Unfortunately, the HLL scheme cannot adequately approximate the contact waves. The goal of the present work is to derive an HLLC type [24,25] contact preserving scheme for (1.6).

The paper is organized as follows. In the next section, basic properties of the system (1.6) are exhibited and a contact preserving scheme is derived. Section 3 is devoted to establish the robustness of the numerical procedure. We prove that the updated radiation state vector remains admissible with a positive radiative energy and a relevant flux limitation. Section 4 deals with the source terms, where a recent procedure developed by Berthon and Turpault [6] is adopted. The obtained numerical scheme is shown to satisfy an asymptotic preserving property and then to restore the diffusive limit equation. In Section 5 , we highlight the interest of the scheme by performing several numerical experiments. A conclusion completes the present work.

2   A contact preserving scheme

According to the pioneer work by Toro [24,25], we here propose to develop a numerical scheme able to capture the stationary contact waves. For the sake of simplicity in the scheme derivation, the following numerical developments are performed involving the model in the x-direction. Let us note from now on that such an assumption is not restrictive since the numerical experiments will be performed on Cartesian grids. As a consequence, the system under consideration reads as follows

$$\begin{cases} \partial_t E + \partial_x F_x = 0, \\ \partial_t F_x + c^2 \partial_x P_{xx} = 0, \\ \partial_t F_y + c^2 \partial_x P_{xy} = 0, \end{cases} \tag{2.1}$$

where P_{xx} and P_{xy} are defined from the radiative pressure (1.4) by

$$P_{xx} = \left(\frac{1 - \chi(f)}{2} + \frac{3\chi(f) - 1}{2}\frac{\mathbf{F}_x^2}{\|\mathbf{F}\|^2}\right)E, \tag{2.2}$$

$$P_{xy} = \left(\frac{3\chi(f) - 1}{2}\frac{\mathbf{F}_x\mathbf{F}_y}{\|\mathbf{F}\|^2}\right)E. \tag{2.3}$$

It turns out to be convenient to introduce several notations. We set

$$\Pi = \frac{1 - \chi(f)}{2}E, \tag{2.4}$$

$$\beta_x = \frac{3\chi(f) - 1}{2}\frac{F_x}{\|\mathbf{F}\|^2}cE, \tag{2.5}$$

to rewrite (2.1) in the following form

$$\begin{cases} \partial_t E + \partial_x F_x = 0, \\ \partial_t F_x + \partial_x(c\beta_x F_x + c^2\Pi) = 0, \\ \partial_t F_y + \partial_x(c\beta_x F_y) = 0. \end{cases} \tag{2.6}$$

In the sequel and for the sake of simplicity in the notations, we set $U=(E, F_x, F_y)^T$ and we define the flux function as follows

$$\mathcal{F} = \left(F_x, c^2 P_{xx}, c^2 P_{xy}\right)^T = \left(F_x, c\beta_x F_x + c^2\Pi, c\beta_x F_y\right)^T.$$

Before we start considering the development of the required scheme, with benefit, we use the formulation (2.6) of the M_1 model to characterize the contact wave solutions.

Lemma 2.1. *The system of conservation laws* (2.6) *is hyperbolic over the open set $\mathring{A}$. It admits three ordered eigenvalues noted $\lambda^\pm$ and λ^0 with*

$$-c < \lambda^- < \lambda^0 < \lambda^+ < c. \tag{2.7}$$

The fields associated with $\lambda^\pm$ are genuinely nonlinear, while the field associated with $\lambda^0 = c\beta_x$ is linearly degenerate. The two Riemann invariants coming from the linearly degenerate field are Π and β_x, respectively defined by (2.4) *and* (2.5).

Proof. We refer to [12] where the author establish the hyperbolic property of (2.6) and give the nature of the fields. Now we have to show that Π and β_x remain continuous across a constant wave. To address such an issue, let us consider a discontinuous solution, which discontinuity propagates at velocity s, made of two constant states U_L and U_R in $\mathcal{A}$. From the Rankine-Hugoniot relations, the triplet $(s; U_L, U_R)$ satisfies

$$-s[E] + [F_x] = 0, \tag{2.8}$$

$$-s[F_x] + [c\beta_x F_x + c^2\Pi] = 0, \tag{2.9}$$

$$-s[F_y] + [c\beta_x F_y] = 0, \tag{2.10}$$

where $[X]=X_R - X_L$ denotes the jump across the discontinuity. We immediately satisfy the jump relation (2.9) and (2.10) as soon as we have

$$s = (\beta_x)_L = (\beta_x)_R, \quad \text{and} \quad \Pi_L = \Pi_R. \tag{2.11}$$

Next, involving (2.4)-(2.5) let us note that the following relation holds

$$F_x = c\beta_x E + c\beta_x \Pi,$$

to deduce that the first jump relation (2.8) is also satisfied. The proof is completed. $\square$
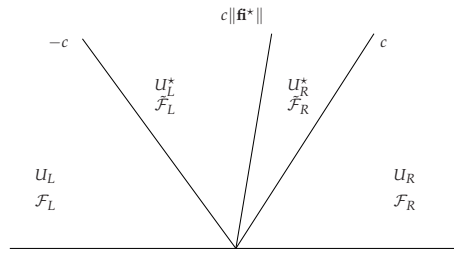

Figure 1: Approximate Riemann solver of HLLC-type.

We now approximate the Riemann solution of (2.6). We propose to consider an approximate Riemann solver in the following form (see [2, 17, 24, 25] to further details and Fig. 1):

$$U^{\mathcal{R}}(x/t; U_L, U_R) = \begin{cases} U_L, & \text{if } x/t < -c, \\ U_L^\star, & \text{if } -c < x/t < c\beta_x^\star, \\ U_R^\star, & \text{if } c\beta_x^\star < x/t < c, \\ U_R, & \text{if } x/t > c, \end{cases} \tag{2.12}$$

where the wave speed $c\beta^\star$ will be proved to be in $(-c, c)$ later on.

We have to evaluate the intermediate states $U_L^\star$ and $U_R^\star$, and the associated approximate flux functions $\tilde{\mathcal{F}}_L$ and $\tilde{\mathcal{F}}_R$. To access such an issue, after Harten-Lax-Van Leer [17], Rankine-Hugoniot like conditions are considered across each wave with speed c to write

$$\begin{cases} -c(U_L^\star - U_L) = \tilde{\mathcal{F}}_L - \mathcal{F}(U_L), \\ c(U_R^\star - U_R) = \tilde{\mathcal{F}}_R - \mathcal{F}(U_R). \end{cases} \tag{2.13}$$

Several supplementary conditions have to be considered. After Toro [24, 25] (see also [4,7]), we enforce the continuity of the Riemann invariant across the middle wave with velocity $c\beta_x^\star$. Hence, we have

$$\begin{cases} (\beta_x)_L^\star = (\beta_x)_R^\star = \beta_x^\star, \\ \Pi_L^\star = \Pi_R^\star = \Pi^\star. \end{cases} \tag{2.14}$$

We complete the system to be solved by several linearizations, which retranscribe the relations linking the Riemann invariants (β_x, Π) and the radiative state vector U. Then

we set

$$
\begin{cases}
F^\star_{x,L} = \tilde{F}_{x,L} = c\beta^\star_x(E^\star_L + \Pi^\star), \\
F^\star_{y,L} = \tilde{F}_{y,L}, \\
\tilde{P}_{xx,L} = \dfrac{\beta^\star_x \tilde{F}_{x,L}}{c} + \Pi^\star, \\
\tilde{P}_{xy,L} = \dfrac{\beta^\star_x \tilde{F}_{y,L}}{c},
\end{cases}
\qquad
\begin{cases}
F^\star_{x,R} = \tilde{F}_{x,R} = c\beta^\star_x(E^\star_R + \Pi^\star), \\
F^\star_{y,R} = \tilde{F}_{y,R}, \\
\tilde{P}_{xx,R} = \dfrac{\beta^\star_x \tilde{F}_{x,R}}{c} + \Pi^\star, \\
\tilde{P}_{xy,R} = \dfrac{\beta^\star_x \tilde{F}_{y,R}}{c}.
\end{cases}
\tag{2.15}
$$

Now, the unknowns $U^\star_{L,R}$, $\tilde{F}_{L,R}$ and $(\beta^\star_x, \Pi^\star)$ are solution of the system made of (2.13) and (2.15). As a consequence, the approximate Riemann solver (2.12) is fully characterized as soon as the system (2.13)-(2.15) is solved. To simplify the formulas in the following, we introduce convenient notations

$$
E^{\star,HLL} = \frac{cE_R + cE_L - (F_{x,R} - F_{x,L})}{2c}, \tag{2.16a}
$$

$$
F^{\star,HLL}_x = \frac{F_{x,R} + F_{x,L} - c(P_{xx,R} - P_{xx,L})}{2}, \tag{2.16b}
$$

$$
\tilde{F}^{HLL}_x = \frac{F_{x,L} + F_{x,R} - c(E_R - E_L)}{2}, \tag{2.16c}
$$

$$
\tilde{P}^{HLL}_{xx} = \frac{cP_{xx,L} + cP_{xx,R} - (F_{x,R} - F_{x,L})}{2c}. \tag{2.16d}
$$

We note that these notations coincide with the single intermediate state vector and its associated approximate flux function involved in the HLL Riemann solver [17]. The detail of this remark is out of our purpose and the reader is referred to [4,7,9,19,24] (and references therein) for complementary features.

We now detail the solution of (2.13)-(2.15). In the next statement we evaluate the unknowns which determine the considered approximate Riemann solver.

Theorem 2.1. *Assume U_L and U_R to be given in $\mathcal{A}$. The unknown $\beta^\star_x$ is the single solution in $(-1,1)$ of the following quadratic equation*

$$
\beta^{\star 2}_x \tilde{F}^{HLL}_x - c(\tilde{P}^{HLL}_{xx} + E^{\star,HLL})\beta^\star_x + F^{\star,HLL}_x = 0. \tag{2.17}
$$

Next, $\Pi^\star$ is given by

$$
\Pi^\star = \tilde{P}^{HLL}_{xx} - \frac{\beta^\star_x}{c} F^{\star,HLL}_x. \tag{2.18}
$$

The intermediate radiative energies are defined as follows

$$
E^\star_L = \frac{1}{1 + \beta^\star_x}\left(E_L - \beta^\star_x \Pi^\star + \frac{F_{x,L}}{c}\right), \tag{2.19a}
$$

$$
E^\star_R = \frac{1}{1 - \beta^\star_x}\left(E_R + \beta^\star_x \Pi^\star - \frac{F_{x,R}}{c}\right). \tag{2.19b}
$$

The unknowns $F_{x,L,R}^{\star}$, $\tilde{F}_{x,L,R}$, $\tilde{P}_{xx,L,R}$ and $\tilde{P}_{xy,L,R}$ are defined by (2.15), while $F_{y,L,R}^{\star}$ is given by

$$F_{y,L}^{\star} = F_{y,L} - c(\tilde{P}_{xy,L} - P_{xy,L}), \quad \text{and} \quad F_{y,R}^{\star} = F_{y,R} + c(\tilde{P}_{xy,R} - P_{xy,R}). \tag{2.20}$$

The proof of this theorem is detailed in the appendix.

After the work of Harten-Lax-Van Leer [17], we use the obtained approximate Riemann solver (2.12) to derive a Godunov-type scheme. We consider a uniform mesh defined by the cell $[x_{i-1/2}, x_{i+1/2})$, where $x_{i+1/2} = x_i + \Delta x/2$, for all i in $\mathbb{Z}$ with a constant increment Δx. The time discretization is given by $t^{n+1} = t^n + \Delta t$, where Δt is restricted according to a CFL like condition given by (according to (2.7))

$$c\frac{\Delta t}{\Delta x} \leq \frac{1}{2}. \tag{2.21}$$

As usual, at the time t^n, we assume to be known a piecewise constant approximation of $U(x, t^n)$ defined as follows

$$U^h(x, t^n) = U_i^n, \quad \text{if} \quad x \in \left[x_{i-\frac{1}{2}}, x_{i+\frac{1}{2}}\right).$$

At each cell interface $x_{i+1/2}$, we set the approximate Riemann solver defined by (2.12) with $U_L = U_i^n$, and $U_R = U_{i+1}^n$. Under the CFL restriction (2.21), we thus consider a juxtaposition of non-interacting Riemann solvers (see Fig. 2), denoted $U^h(x, t^n + t)$ for $t \in [0, \Delta t)$.
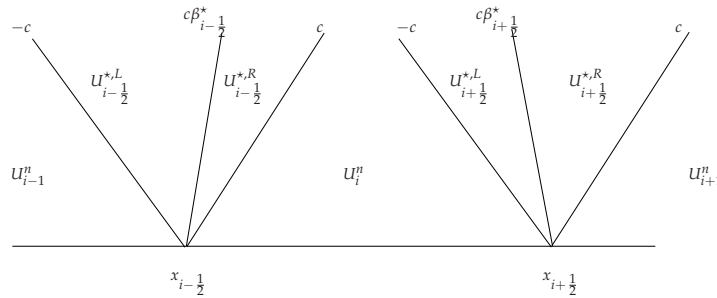
Figure 2: Successive Riemann problems.

The updated state vector is obtained as follows

$$\begin{aligned} U_{i+1}^n &= \frac{1}{\Delta x} \int_{x_{i-\frac{1}{2}}}^{x_{i+\frac{1}{2}}} U^h(x, t^n + \Delta t) dx \\ &= \frac{1}{\Delta x} \int_{x_{i-\frac{1}{2}}}^{x_i} U^{\mathcal{R}}\left(\frac{x - x_{i-\frac{1}{2}}}{\Delta t}; U_{i-1}^n, U_i^n\right) dx \\ &\quad + \frac{1}{\Delta x} \int_{x_i}^{x_{i+\frac{1}{2}}} U^{\mathcal{R}}\left(\frac{x - x_{i+\frac{1}{2}}}{\Delta t}; U_i^n, U_{i+1}^n\right) dx. \end{aligned} \tag{2.22}$$

A standard computation gives the following detailed scheme

$$E_i^{n+1} = E_i^n - \frac{\Delta t}{\Delta x}\left(\mathcal{F}_{i+\frac{1}{2}}^E - \mathcal{F}_{i-\frac{1}{2}}^E\right), \tag{2.23a}$$

$$(F_x)_i^{n+1} = (F_x)_i^n - \frac{\Delta t}{\Delta x}\left(\mathcal{F}_{i+\frac{1}{2}}^{F_x} - \mathcal{F}_{i-\frac{1}{2}}^{F_x}\right), \tag{2.23b}$$

$$(F_y)_i^{n+1} = (F_y)_i^n - \frac{\Delta t}{\Delta x}\left(\mathcal{F}_{i+\frac{1}{2}}^{F_y} - \mathcal{F}_{i-\frac{1}{2}}^{F_y}\right), \tag{2.23c}$$

where we have set the notations as

$$\mathcal{F}_{i+\frac{1}{2}}^E = \begin{cases} c(\beta_x^\star)_{i+\frac{1}{2}}\left(E_{i+\frac{1}{2}}^{\star,L} + \Pi_{i+\frac{1}{2}}^\star\right), & \text{if } (\beta_x^\star)_{i+\frac{1}{2}} > 0, \\ c(\beta_x^\star)_{i+\frac{1}{2}}\left(E_{i+\frac{1}{2}}^{\star,R} + \Pi_{i+\frac{1}{2}}^\star\right), & \text{otherwise,} \end{cases} \tag{2.24a}$$

$$\mathcal{F}_{i+\frac{1}{2}}^{F_x} = \Pi_{i+\frac{1}{2}}^\star + \frac{(\beta_x^\star)_{i+\frac{1}{2}}}{c}\mathcal{F}_{i+\frac{1}{2}}^E, \tag{2.24b}$$

$$\mathcal{F}_{i+\frac{1}{2}}^{F_y} = \begin{cases} \frac{(\beta_x^\star)_{i+\frac{1}{2}}}{1+(\beta_x^\star)_{i+\frac{1}{2}}}\left((P_{xy})_i^n + \frac{(F_y)_i^n}{c}\right), & \text{if } (\beta_x^\star)_{i+\frac{1}{2}} > 0, \\ \frac{-(\beta_x^\star)_{i+\frac{1}{2}}}{1-(\beta_x^\star)_{i+\frac{1}{2}}}\left((P_{xy})_{i+1}^n + \frac{(F_y)_{i+1}^n}{c}\right), & \text{otherwise.} \end{cases} \tag{2.24c}$$

For the sake of completeness, let us recall that $(\beta_x^\star)_{i+1/2}$ is the unique solution in $(-1,1)$ of the following equation

$$X^2(\tilde{F}_x^{HLL})_{i+\frac{1}{2}} - c\left((\tilde{P}_{xx}^{HLL})_{i+\frac{1}{2}} + (E^{\star,HLL})_{i+\frac{1}{2}}\right)X + (F_x^{\star,HLL})_{i+\frac{1}{2}} = 0,$$

where we have set

$$\Pi_{i+\frac{1}{2}}^\star = (\tilde{P}_{xx}^{HLL})_{i+\frac{1}{2}} - \frac{(\beta_x^\star)_{i+\frac{1}{2}}}{c}(\tilde{F}_x^{HLL})_{i+\frac{1}{2}}, \tag{2.25a}$$

$$E_{i+\frac{1}{2}}^{\star,L} = \frac{1}{1+(\beta_x^\star)_{i+\frac{1}{2}}}\left(E_i^n - (\beta_x^\star)_{i+\frac{1}{2}}\Pi_{i+\frac{1}{2}}^\star + \frac{(F_x)_i^n}{c}\right), \tag{2.25b}$$

$$E_{i+\frac{1}{2}}^{\star,R} = \frac{1}{1-(\beta_x^\star)_{i+\frac{1}{2}}}\left(E_{i+1}^n + (\beta_x^\star)_{i+\frac{1}{2}}\Pi_{i+\frac{1}{2}}^\star + \frac{(F_x)_{i+1}^n}{c}\right), \tag{2.25c}$$

with the notations

$$E_{i+\frac{1}{2}}^{\star,HLL} = \frac{cE_{i+1}^n + cE_i^n - \left((F_x)_{i+1}^n - (F_x)_i^n\right)}{2c}, \tag{2.26a}$$

$$(F_x^{\star,HLL})_{i+\frac{1}{2}} = \frac{(F_x)_{i+1}^n + (F_x)_i^n - c\left((P_{xx})_{i+1}^n - (P_{xx})_i^n\right)}{2}, \tag{2.26b}$$

$$(\tilde{F}_x^{HLL})_{i+\frac{1}{2}} = \frac{(F_x)_i^n + (F_x)_{i+1}^n - c(E_{i+1}^n - E_i^n)}{2}, \tag{2.26c}$$

$$(\tilde{P}_{xx}^{HLL})_{i+\frac{1}{2}} = \frac{c(P_{xx})_i^n + c(P_{xx})_{i+1}^n - \left((F_x)_{i+1}^n - (F_x)_i^n\right)}{2c}. \tag{2.26d}$$

The derivation of the contact preserving scheme to approximate the weak solution of (2.1) is thus completed.

3   Properties of the scheme

In the present section, we exhibit the main properties satisfied by the scheme. We establish that the scheme preserves the admissible states. In addition, we show the accuracy of the method when evaluating contact discontinuities.

First we prove that the considered numerical procedure, defined by (2.23)-(2.26), ensures the positiveness of the radiative energy and the radiative flux limitation.

Theorem 3.1. *Consider an admissible sequence* $(U_i^n)_{i \in \mathbb{Z}}$ *in* $\mathcal{A}$. *Assume that the CFL condition* (2.21) *holds, and define the updated sequence* $(U_i^{n+1})_{i \in \mathbb{Z}}$ *by the scheme* (2.23)-(2.26). *Then we have* $(U_i^{n+1}) \in \mathcal{A}$, *for all* $i \in \mathbb{Z}$.

The proof of this statement easily comes from the following property concerning the approximate Riemann solver.

Lemma 3.1. *Let* U_L *and* U_R *be given in* $\mathcal{A}$. *Consider the approximate Riemann solver* $U^{\mathcal{R}}$ *defined by* (2.12) *and Theorem* 2.1. *Then* $U^{\mathcal{R}}$ *remains in* $\mathcal{A}$, *for all* $t > 0$ *and* $x \in \mathbb{R}$.

The proof of the robustness of the approximate Riemann solver will be given at the end of this section.

Proof of Theorem 3.1. Arguing Lemma 3.1, the juxtaposition of the non-interacting Riemann solvers $U^h(x, t)$ remains in $\mathcal{A}$, for all $t \in [t^n, t^n + \Delta t]$. The definition of the updated states U_i^{n+1}, given by (2.22), completes the proof. $\square$

Now, let us carry on considering the accuracy of the scheme. Indeed, in the following result, the scheme (2.23)-(2.26) is proved to preserve the stationary contact waves.

Theorem 3.2. *Consider an admissible sequence* $(U_i^n)_{i \in \mathbb{Z}}$ *in* $\mathcal{A}$. *For all* i *in* $\mathbb{Z}$, *assume* $(\beta_x)_i^n = 0$, *where* $(\beta_x)_i^n = \beta_x(U_i^n)$ *is defined by* (2.5). *Let us set* Π *a positive constant. Assume* $\Pi_i^n = \Pi$, *for all* $i \in \mathbb{Z}$, *where* $\Pi_i^n = \Pi(U_i^n)$ *is given by* (2.4). *Then we have* $U_i^{n+1} = U_i^n$, *for all* $i \in \mathbb{Z}$.

This result is a direct consequence of the property of the approximate Riemann solver to exactly capture the stationary contact discontinuity.

Lemma 3.2. *Let* U_L *and* U_R *be given in* $\mathcal{A}$, *and assume that* U_L *and* U_R *define a stationary contact wave; namely* $(\beta_x)_L = (\beta_x)_R = 0$ *and* $\Pi_L = \Pi_R$. *Then the approximate Riemann solver, defined by* (2.12) *and Theorem* 2.1, *coincides with the exact stationary contact wave solution*

$$U^{\mathcal{R}}(x/t; U_L, U_R) = \begin{cases} U_L, & \text{if} \quad x/t < 0, \\ U_R, & \text{if} \quad x/t > 0. \end{cases}$$

Proof. Arguing the definition of β_x, given by (2.5), as soon as $\beta_x = 0$, we have $F_x = 0$. As a consequence $(F_x)_L = (F_x)_R = 0$. In addition, the radiative pressure reads

$$(P_{xx})_L = (P_{xx})_R = \Pi,$$
$$(P_{xy})_L = (P_{xy})_R = 0.$$

From these values and the relation (2.16a), we deduce that $F_x^{\star,HLL}=0$ and $\tilde{P}_{xx}^{HLL}=\Pi$.

We now evaluate the intermediate states of $U^{\mathcal{R}}$. First, $\beta_x^\star$ is the unique solution in $(-1,1)$ of the following equation

$$X^2 \tilde{F}_x^{HLL} - cX\big(\tilde{P}_{xx}^{HLL} + E^{\star,HLL}\big) = 0.$$

Hence, we have $\beta_x^\star=0$. Next, from (2.18), we have $\Pi^\star=\Pi$. Concerning the radiative energy, from (2.19a) and (2.19b), we obtain $E_L^\star=E_L$ and $E_R^\star=E_R$. From (2.15), we get $F_{x,L}^\star=F_{x,R}^\star=0$, while (2.20) gives $F_{y,L}^\star=F_{y,L}$ and $F_{y,R}^\star=F_{y,R}$. The proof is completed. $\quad\square$

Proof of Theorem 3.2. Using Lemma 3.2, the expected result is an immediate consequence of the updated state vector definition (2.22). $\quad\square$

The present section is now concluded by establishing the robustness property satisfied by the approximate Riemann solver.

Proof of Lemma 3.1. We first establish that $U_L^\star \in \mathcal{A}$. To address such an issue, we need a suitable formulation of $E_L^\star$ and $F_L^\star$ as a function of $\beta_x^\star$ given by

$$E_L^\star = E_L \frac{(1+f_L)(\beta_x^\star)^2 + (1-D_{xx,L})\beta_x^\star + 1 + f_{x,L}}{(1+\beta_x^\star)^2}, \tag{3.1}$$

$$F_{x,L}^\star = c\beta_x^\star E_L \frac{(1+f_{x,L})(1+2f_{x,L}+D_{xx,L})}{(1+\beta_x^\star)^2}, \tag{3.2}$$

where, according to the definition (2.2), we have set

$$P_{xx,L} = D_{xx,L}E_L, \quad \text{and} \quad F_{x,L} = cf_{x,L}E_L,$$

with $f_{x,L} \in [-1,1]$, and $D_{xx,L} \in [0,1]$.

To establish these two above relations, from (2.13) and (2.15), let us first recall that the Rankine-Hugoniot conditions across the left discontinuity rewrite as follows

$$F_{x,L}^\star - F_{x,L} = -c(E_L^\star - E_L), \tag{3.3}$$

$$c^2(\tilde{P}_{xx,L} - P_{xx,L}) = -c(F_{x,L}^\star - F_{x,L}), \tag{3.4}$$

$$c^2(\tilde{P}_{xy,L} - P_{xy,L}) = b_L(F_{y,L}^\star - F_{y,L}). \tag{3.5}$$

Since from (2.15), we have

$$F_{x,L}^\star = c\beta_x^\star(E_L^\star + \Pi), \tag{3.6}$$

from (3.3) we deduce

$$E_L^\star = \frac{F_{x,L} + cE_L - c\beta_x^\star\Pi^\star}{c(\beta_x^\star + 1)}. \tag{3.7}$$

Plugging this formulation of $E_L^\star$ in (3.6), we obtain

$$F_{x,L}^\star = \beta_x^\star \frac{F_{x,L} + cE_L + c\Pi^\star}{\beta_x^\star + 1}. \tag{3.8}$$

Using $\tilde{P}_{xx,L} = \beta_x^\star F_{x,L}^\star/c + \Pi^\star$ in (3.4), we can deduce from (3.8) that

$$\Pi^\star = \frac{F_{x,L} + cP_{xx,L} - \beta_x^\star(F_{x,L} + cE_L)}{c(\beta_x^\star + 1)}, \tag{3.9}$$

and by replacing the value of $\Pi^\star$ in (3.7) and (3.8), we obtain the required relations (3.1) and (3.2).

We now prove the non negativity of $E_L^\star$. Since $|\beta_x^\star| < 1$, we can deduce from (3.1) that $E_L^\star \geq 0$ if and only if the second order polynomial in $\beta_x^\star$, given by

$$\varphi(\beta_x^\star) = (1 + f_{x,L})(\beta_x^\star)^2 + (1 - D_{xx,L})\beta_x^\star + 1 + f_{x,L},$$

is non negative. First, let us note that $f_{x,L} = -1$, implies $f_{y,L} = 0$. Since we have

$$f_{x,L}^2 + f_{y,L}^2 \leq 1.$$

Then we deduce $\varphi(\beta_x^\star)|_{\{f_{x,L}=-1\}} = 0$ to write $E_L^\star|_{\{f_{x,L}=-1\}} = 0$. Now, we assume $f_{x,L} \in (-1, 1]$ to note that the highest order coefficient is positive. As a consequence, it will be sufficient to show that the discriminant of φ is non positive. This discriminant can be factorized as follows

$$(1 - D_{xx,L})^2 - 4(1 + f_{x,L})^2 = -(1 + 2f_{x,L} + D_{xx,L})(3 + 2f_{x,L} - D_{xx,L}).$$

Since we have $(1 \pm 2f_{x,L} + D_{xx,L}) \geq 0$ from Lemma A.3, and $(3 + 2f_{x,L} - D_{xx,L}) \geq 0$ from $-1 \leq f_{x,L} \leq 1$ and $0 \leq D_{xx,L} \leq 1$, we obtain

$$(1 - D_{xx,L})^2 - 4(1 + f_{x,L})^2 \leq 0,$$

and thus we have

$$\varphi(\beta_x^\star) \geq 0.$$

Hence the left intermediate energy $E_L^\star$ is non negative.

To prove the flux limitation of left state, i.e., $-cE_L^\star \leq F_L^\star \leq cE_L^\star$, we introduce the variable $\delta_L^\star$ defined by

$$\delta_L^\star = c(E_L^\star)^2 - (F_{x,L}^\star)^2 - (F_{y,L}^\star)^2,$$

to write the flux limitation property in the equivalent form $\delta_L^\star \geq 0$. Now, we establish that $\delta_L^\star \geq 0$.

Since $\tilde{P}_{xy,L} = \beta_x^\star F_{y,L}^\star/c$, we can deduce from (3.5) that

$$F_{y,L}^\star = c\frac{F_{y,L} + P_{xy,L}}{1 + \beta_x^\star} = cE_L\frac{f_{y,L} + D_{xy,L}}{1 + \beta_x^\star}, \tag{3.10}$$

where $P_{xy,L} = D_{xy,L}E_L$, and $F_{y,L} = cf_{y,L}E_L$ with $f_{y,L} \in [-1, 1]$, and $D_{xy,L} \in [-1, 1]$. Using (3.7), (3.8) and (3.10), the quantity $\delta_L^\star$ can be written as

$$\delta_L^\star = c^2 E_L^2\frac{\phi(\beta_x^\star)}{(1 + \beta_x^\star)^2},$$

where

$$\phi(\beta_x^\star) = (1 + f_{x,L})^2 (\beta_x^\star)^2 - 2(1 + f_{x,L})(f_{x,L} + D_{xx,L})\beta_x^\star$$
$$+ (1 + f_{x,L})^2 - (f_{y,L} + D_{xy,L})^2.$$

Therefore, the sign of $\delta_L^\star$ is given by the sign of the second order polynomial ϕ. First, let us note that $\phi(\beta_x^\star)=0$ as soon as $f_{x,L}=-1$, and then we have

$$\delta_L^\star\big|_{\{f_{x,L}=-1\}}= 0.$$

Next, we assume $f_{x,L}=-1$ to have the highest order coefficient $(1 + f_{x,L})^2$ positive. As a consequence, the expected flux limitation will be established as soon as the reduced discriminant associated with ϕ is non positive. This reduced discriminant Δ' can be written as

$$\Delta' = (1 + f_{x,L})^2\delta,$$
$$\delta = (f_{x,L} + D_{xx,L})^2 + (f_{y,L} + D_{xy,L})^2 - (1 + f_{x,L})^2.$$

Hence, the left state is flux limited if δ is non positive. Using the expression of $D_{xx,L}$ and $D_{xy,L}$, we get

$$D_{xx,L} = \frac{(1 - \chi_L)}{2} + \frac{(3\chi_L - 1)}{2}\frac{f_{x,L}^2}{f_L^2}, \quad D_{xy,L} = \frac{(3\chi_L - 1)}{2}\frac{f_{x,L}f_{y,L}}{f_L^2},$$

where we have set $\chi_L=\chi(f_L)$ with χ defined by (1.5), and $f_L=(f_{x,L}^2 + f_{y,L}^2)^{1/2}$. For all $\theta \in (-\pi, \pi)$, let us set

$$f_{x,L} = f_L \cos(\theta), \quad \text{and} \quad f_{y,L} = f_L \sin(\theta),$$

to write δ in the following form

$$\delta = \frac{1}{4}\Big((3\chi_L^2 + 2\chi_L - 1 - 4f_L^2) \cos(\theta)^2 + 8f_L(\chi_L - 1) \cos(\theta)$$
$$+ (4f_L^2 + \chi_L^2 - 2\chi_L - 3)\Big),$$

which is a second order polynomial in $\cos(\theta)$. From a basic function analysis, the highest coefficient of this polynomial is negative for $f_L\in(0,1)$, and it vanishes for $f_L=0$ and $f_L=1$. From an easy calculation, we have

$$\delta\big|_{\{f_L=0\}}= -\frac{32}{9}, \quad \text{and} \quad \delta\big|_{\{f_L=1\}}= 0.$$

Now, let us consider $f_L\in(0,1)$ to write the associated reduced discriminant of this polynomial as follows

$$\Delta'' = -(\chi_L + 2f_L + 1)(\chi_L - 2f_L + 1)(3\chi_L^2 - 10\chi_L + 4f_L^2 + 3).$$

By the definition of χ, given by (1.5), the third coefficient is equal to zero, hence we have $\Delta''=0$. As a consequence, $\delta \leq 0$ and we have proved that the left state $U_L^\star$ is flux limited. The proof concerning the right state $U_R^\star$ is similar and is omitted here.   □

4   The source terms discretization

We have proposed a finite volume scheme to approximate the solutions of (2.1). This scheme is easily extended to take into account the material temperature which is governed by the stationary equation (omitting the source term)

$$\partial_t(\rho C_v T) = 0.$$

To shorten the notations, we set

$$W = (E, F_x, F_y, \rho C_v T)^T, \quad \text{and} \quad \bar{\mathcal{F}}(W) = (F_x, c^2 P_{xx}, c^2 P_{xy}, 0)^T,$$

to denote the state and flux function vectors. Hence, to approximate the free streaming region associated to the M_1 model, governed by the following system

$$\begin{cases} \partial_t E + \partial_x F_x = 0, \\ \partial_t F_x + \partial_x c^2 P_{xx} = 0, \\ \partial_t F_y + \partial_x c^2 P_{xy} = 0, \\ \partial_t(\rho C_v T) = 0, \end{cases}$$

we have derived the following contact discontinuity preserving scheme given by

$$W_i^{n+1} = W_i^n - \frac{\Delta t}{\Delta x}\left(\bar{\mathcal{F}}_{i+\frac{1}{2}} - \bar{\mathcal{F}}_{i-\frac{1}{2}}\right), \tag{4.1a}$$

$$\bar{\mathcal{F}}_{i+\frac{1}{2}} = \left(\mathcal{F}_{i+\frac{1}{2}}^E, \mathcal{F}_{i+\frac{1}{2}}^{F_x}, \mathcal{F}_{i+\frac{1}{2}}^{F_y}, 0\right)^T, \tag{4.1b}$$

where the formulas (2.24)-(2.26) are used.

Now, we propose to modify this method to introduce a suitable discretization of the source term in order to approximate the system

$$\begin{cases} \partial_t E + \partial_x F_x = c\sigma(aT^4 - E), \\ \partial_t F_x + \partial_x c^2 P_{xx} = -c\sigma F_x, \\ \partial_t F_y + \partial_x c^2 P_{xy} = -c\sigma F_y, \\ \partial_t(\rho C_v T) = -c\sigma(aT^4 - E), \end{cases} \tag{4.2}$$

For the sake of simplicity in the forthcoming developments, we set

$$\mathcal{F}(W) = (F_x, c^2 P_{xx}, c^2 P_{xy}, 0)^T.$$

To take into account the source term, we introduce it inside the Riemann solver using a technique derived in [6]. Such a modification yields to a consistant scheme which degenerates into a diffusion equation when σ is large. However, this limit diffusion equation is not the expected equilibrium diffusion equation (1.8). To recover (1.8), we

introduce a suitable correction parameter $\bar{\sigma} \geq 0$ and rewrite the system in the equivalent following form

$$
\begin{cases}
c\sigma(aT^4 - E) = c(\sigma + \bar{\sigma})\left(\frac{\sigma}{\sigma+\bar{\sigma}}aT^4 + \frac{\bar{\sigma}}{\sigma+\bar{\sigma}}E - E\right), \\
-c\sigma F_x = c(\sigma + \bar{\sigma})\left(\frac{\bar{\sigma}}{\sigma+\bar{\sigma}}F_x - F_x\right), \\
-c\sigma F_y = c(\sigma + \bar{\sigma})\left(\frac{\bar{\sigma}}{\sigma+\bar{\sigma}}F_y - F_y\right), \\
-c\sigma(aT^4 - E) = c(\sigma + \bar{\sigma})\left(\frac{\sigma}{\sigma+\bar{\sigma}}(E + \rho C_v T - aT^4 + \frac{\bar{\sigma}}{\sigma+\bar{\sigma}}\rho C_v T - \rho C_v T\right).
\end{cases}
$$

From a numerical point of view, $\bar{\sigma}$ can participate to control the numerical viscosity (see [6] for further details).

To simplify the notations let us set

$$
R(W) = (aT^4, 0, 0, E + \rho C_v T - aT^4)^T,
$$

$$
\bar{R}(W) = \frac{\bar{\sigma}}{\sigma + \bar{\sigma}}R(W) + \frac{\bar{\sigma}}{\sigma + \bar{\sigma}}W,
$$

to write (4.2) in the following condensed form

$$
\partial_t W + \partial_x \bar{\mathcal{F}}(W) = c(\sigma + \bar{\sigma})\left(\bar{R}(W) - W\right).
$$

Next, we correct the approximate Riemann solver $U^{\mathcal{R}}$, defined by (2.12) and Theorem 2.1, by introducing the function $\bar{R}$ as follows

$$
\tilde{W}^{\mathcal{R}}(x,t) = \begin{cases}
W_L, & \text{if} \quad x/t < -c, \\
\alpha W_L^\star + (1-\alpha)\bar{R}^-(W_L), & \text{if} \quad -c < x/t < c\beta_x^\star, \\
\alpha W_R^\star + (1-\alpha)\bar{R}^+(W_R), & \text{if} \quad c\beta_x^\star < x/t < c, \\
W_R, & \text{if} \quad x/t > c,
\end{cases}
$$

where we have set

$$
W_{L,R} = (U_{L,R}, T_{L,R})^T, \qquad W_{L,R}^\star = (U_{L,R}^\star, T_{L,R})^T,
$$

$$
\alpha = \frac{2}{2 + (\sigma + \bar{\sigma})\Delta x}, \qquad \bar{R}^\pm(W_{L,R}) = \frac{\sigma}{\sigma + \bar{\sigma}^\pm}R(W_{L,R}) + \frac{\bar{\sigma}^\pm}{\sigma + \bar{\sigma}^\pm}W_{L,R}.
$$

We adopt this new approximate Riemann solver to define a Godunov type scheme. We then consider the juxtaposition, denoted $W^h(x, t^n + t)$ for $t \in [0, \Delta t]$, of the Riemann solver stated at each interface $x_{i+1/2}$.

The updated state vector is therefore defined as follows

$$
W_i^{n+1} = \frac{1}{\Delta x}\int_{x_{i-\frac{1}{2}}}^{x_{i+\frac{1}{2}}} W^h(x, t^n + \Delta t)dx.
$$

We skip the details of the computation (see [6]), and the resulting scheme reads

$$
\begin{aligned}
W_i^{n+1} = W_i^n &- \frac{\Delta t}{\Delta x}\left(\alpha_{i+\frac{1}{2}}\bar{\mathcal{F}}_{i+\frac{1}{2}} - \alpha_{i-\frac{1}{2}}\bar{\mathcal{F}}_{i-\frac{1}{2}}\right) \\
&+ \Delta t\left(\frac{\sigma + \bar{\sigma}_{i-\frac{1}{2}}}{2 + (\sigma + \bar{\sigma}_{i-\frac{1}{2}})}S_{i-\frac{1}{2}}^+ + \frac{\sigma + \bar{\sigma}_{i+\frac{1}{2}}}{2 + (\sigma + \bar{\sigma}_{i+\frac{1}{2}})}S_{i+\frac{1}{2}}^-\right),
\end{aligned}
$$

where

$$S^-_{i+\frac{1}{2}} = c\big(\bar{R}^-(W^n_i) - W^n_i\big) - \bar{\mathcal{F}}(W^n_i),$$

$$S^+_{i+\frac{1}{2}} = c\big(\bar{R}^+(W^n_{i+1}) - W^n_{i+1}\big) + \bar{\mathcal{F}}(W^n_{i+1}),$$

$$\bar{R}^-(W^n_i) = \frac{\sigma}{\sigma + \bar{\sigma}_{i-\frac{1}{2}}} R(W^n_i) + \frac{\bar{\sigma}_{i-\frac{1}{2}}}{\sigma + \bar{\sigma}_{i-\frac{1}{2}}} W^n_i,$$

$$\bar{R}^+(W^n_i) = \frac{\sigma}{\sigma + \bar{\sigma}_{i+\frac{1}{2}}} R(W^n_i) + \frac{\bar{\sigma}_{i+\frac{1}{2}}}{\sigma + \bar{\sigma}_{i+\frac{1}{2}}} W^n_i,$$

and

$$\alpha_{i+\frac{1}{2}} = \frac{2}{2 + (\sigma + \bar{\sigma}_{i+\frac{1}{2}})\Delta x}.$$

Now we introduce the rescaling parameter ε, which is also involved in (1.7), in order to obtain the limit equation of the scheme. To do so, we substitute Δt, σ and $\bar{\sigma}_{i+1/2}$ by $\Delta t/\varepsilon$, σ/ε and $\bar{\sigma}_{i+1/2}/\varepsilon$. The rescaled scheme thus reads as follows

$$W^{n+1}_i = W^n_i - \frac{\Delta t}{\Delta x}\left(\alpha^\varepsilon_{i+\frac{1}{2}}\bar{\mathcal{F}}_{i+\frac{1}{2}} - \alpha^\varepsilon_{i-\frac{1}{2}}\bar{\mathcal{F}}_{i-\frac{1}{2}}\right)$$

$$+ \frac{\Delta t}{\varepsilon}\left(\frac{\sigma + \bar{\sigma}_{i-\frac{1}{2}}}{2\varepsilon + (\sigma + \bar{\sigma}_{i-\frac{1}{2}})}S^+_{i-\frac{1}{2}} + \frac{\sigma + \bar{\sigma}_{i+\frac{1}{2}}}{2\varepsilon + (\sigma + \bar{\sigma}_{i+\frac{1}{2}})}S^-_{i+\frac{1}{2}}\right), \qquad (4.3)$$

where

$$\alpha^\varepsilon_{i+\frac{1}{2}} = \frac{2}{2\varepsilon + (\sigma + \bar{\sigma}_{i+\frac{1}{2}})\Delta x}.$$

Next, we study the behavior of this rescaled scheme (4.3), as ε tends to zero. In this limit, we have

$$S^+_{i-\frac{1}{2}} + S^-_{i+\frac{1}{2}} = 0,$$

which leads to

$$\bar{R}^-(W^n_i) + \bar{R}^+(W^n_i) - 2W^n_i = 0,$$

and hence we have

$$R(W^n_i) - W^n_i = 0.$$

As a consequence, the limit state vector satisfies

$$E^n_i = a(T^n_i)^4, \qquad (F_x)^n_i = 0, \qquad (F_y)^n_i = 0.$$

Finally, the following discrete diffusion equation is obtained

$$(\rho C_v T + aT^4)^{n+1}_i = (\rho C_v T + aT^4)^n_i + c\frac{\Delta t}{\Delta x^2}\left[\frac{(\rho C_v T + aT^4)^n_{i+1} - (\rho C_v T + aT^4)^n_i}{\sigma + \bar{\sigma}_{i+\frac{1}{2}}}\right.$$

$$\left. + \frac{(\rho C_v T + aT^4)^n_{i-1} - (\rho C_v T + aT^4)^n_i}{\sigma + \bar{\sigma}_{i-\frac{1}{2}}}\right].$$

Remark 4.1. Let us emphasize that the scheme without correction (i.e., $\bar{\sigma} = 0$) is clearly not consistant with the required equilibrium diffusion equation (1.8). Indeed, in this case, the scheme degenerates into a parabolic equation which diffusion coefficient is c/σ instead of $c/3\sigma$ as prescribed in (1.8).

Hopefully, the expected limit equation (1.8) may be recovered involving a suitable choice of the free parameter $\bar{\sigma}_{i+1/2}$. One possibility is to choose

$$
\bar{\sigma}_{i+\frac{1}{2}} = \begin{cases} 2\sigma + 3\sigma\rho C_v \dfrac{T_{i+1}^n - T_i^n}{a(T_{i+1}^n)^4 - a(T_i^n)^4}, & \text{if } T_i^n \neq T_{i+1}^n, \\ 2\sigma + 3\sigma\rho C_v \dfrac{1}{4a(T_i^n)^3}, & \text{otherwise,} \end{cases}
$$

to obtain the expected limit diffusion equation in the following discrete form

$$
(\rho C_v T + aT^4)_i^{n+1} = (\rho C_v T + aT^4)_i^n + \frac{\Delta t}{\Delta x^2}\frac{c}{3\sigma}\Big(a(T_{i+1}^n)^4 - 2a(T_i^n)^4 + a(T_{i-1}^n)^4\Big).
$$

5 Numerical experiments

5.1 Marshak wave

The Marshak wave is a one-dimensional test case that focuses on the chronometric behavior of the scheme. The considered slab of material is initially cold and at radiative equilibrium. A heat wave enters the domain and its evolution is observed.

In [27], this test case is used to compare the M_1 model with various diffusion and flux-limited diffusion models. All of these diffusion models predict wrong diffusion speeds, even with the Levermore-Lorentz's [20] flux-limiter which is also based on a minimum entropy assumption, whereas the M_1 model is quite well behaving timewise.

This test case is composed of a slab of material with $x \in [0, 0.1]$m. The mesh is only made of 10 cells in order to have a challenging benchmark. The initial temperature is equal to 300 K and the source on the left side of the domain has a temperature of 1000 K. This source generates a thermal wave propagating into the initially cold medium.

The opacity is assumed to be constant equal to $\sigma = 100$m^{-1} and $\rho C_v = 10^{-4}$Jm^{-3}K^{-1}. Note that in the present slab, the mean free path is equal to $\lambda = 1/\sigma = 0.01$m, which is actually equal to the spatial resolution $\Delta x = 0.01$m. The time step Δt is set according to the CFL condition (2.21). The results are compared to a reference solution obtained by computing the solution of the full radiative transfer equation, which is the kinetic equation associated to the M_1 model (see [22]).

The radiative temperature profiles, observed at $t = 1.33 \times 10^{-7}$s, are shown in Fig. 3. It compares computations carried with both HLL and HLLC schemes, with or without the asymptotic correction denoted "AP".

We clearly see that the HLLC and HLL schemes both give similar results from a chronometric point of view. It is also to note that results without the asymptotic preserving scheme are too fast compared to the reference solution, whereas the use of the
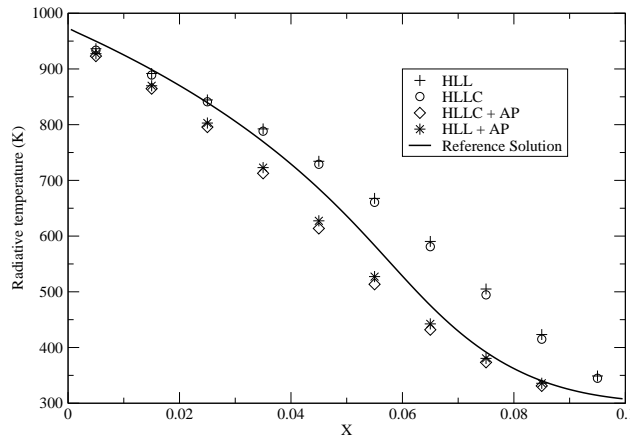
Figure 3: Marshak wave at $t = 1.33 \times 10^{-7}$s.

asymptotic preserving correction allows a much better agreement with the reference solution.

5.2 Shadow cone

Let us now consider a 2D academic test case. It has very stiff initial conditions and intends to demonstrate the quality of the solution provided by the solver. Tests have been performed in [4], and we show here some improvements from the results obtained therein.

We consider the domain $(x, y) \in [0, 2] \times [0, 1]$m as shown on Fig. 4. Computations made here are run on a 80×40 cartesian grid, with a time step Δt fixed by the CFL restriction (2.21). The domain is composed of a dense material ($\rho C_v = 8.6 \times 10^4$Jm^{-3} K^{-1} and $\sigma = 2 \times 10^5$m^{-1}) and a transparent region. A free streaming beam adjacent to the dense material enters the domain through the top left boundary. The other boundaries of the domain are supposed to be transparent. The initial temperature is 1 K in the dense material and 300K elsewhere. A radiative temperature of $T = 5.8 \times 10^6$K
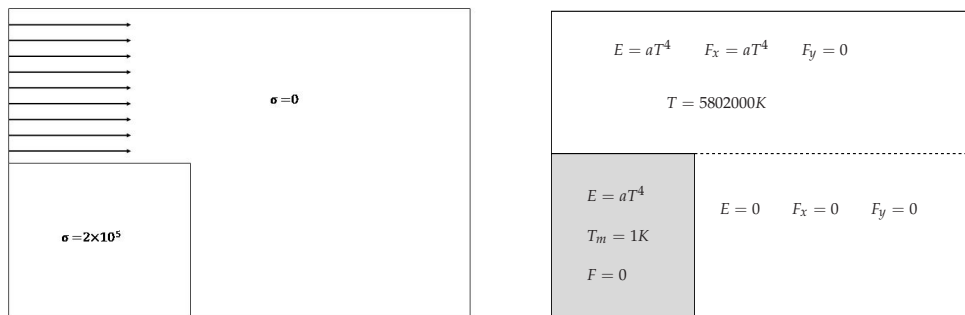

Figure 4: Geometry (left) and exact solution (right) for the 2D case.
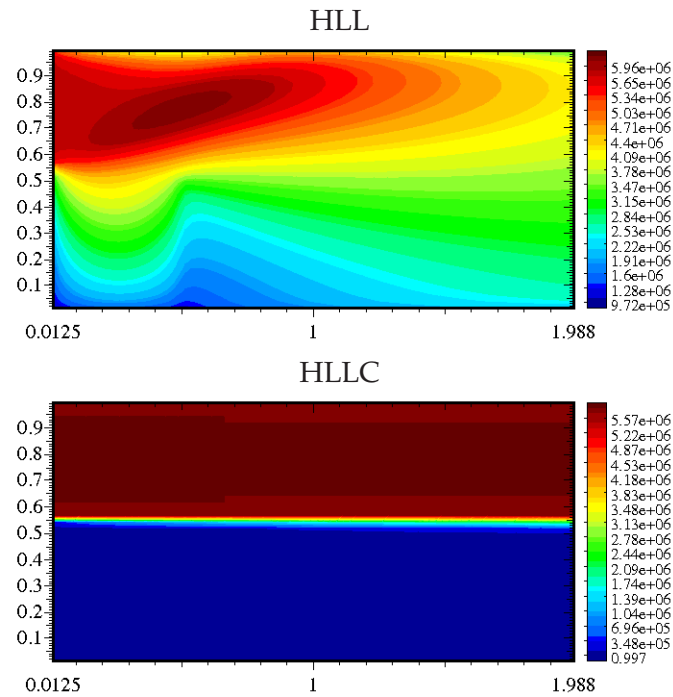
Figure 5: Comparison of the radiative temperature predicted by the HLL scheme (top) with the HLLC (buttom).
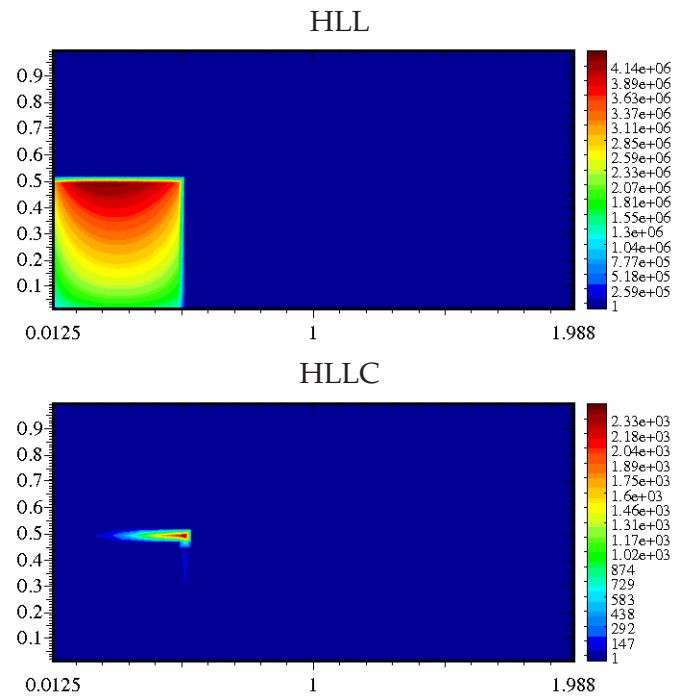

Figure 6: Comparison of the material temperature computed by the HLL scheme (top) with the HLLC (buttom).
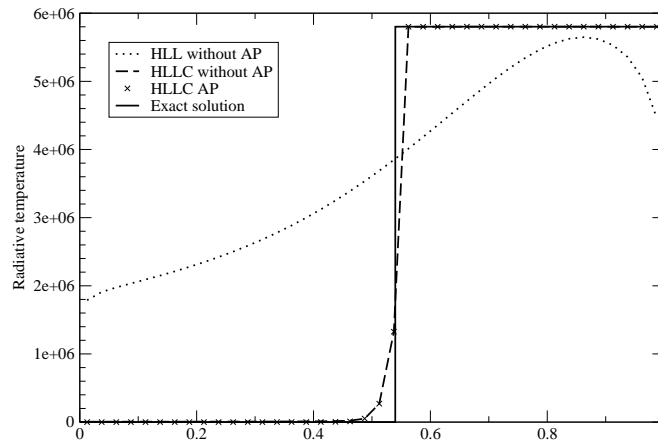
Figure 7: Radiative temperature along the y coordinate (see Fig. 4 for the exact solution).

is applied on the left side of the transparent region (from $y=0.5$m to $y=1$m).

The exact solution is drawn on Fig. 4. Indeed, in the upper part the photons are simply translated from the left boundary to the right of the domain. In the lower part, the solution remains constant against time since no photon enters this area. The line $y=0.5$m is then a stationary contact discontinuity for the M_1-system. The dense material does not get any photon either and its temperature remains constant.

Simulations are stopped at time $t=5 \times 10^{-8}$s. Figs. 5 and 6 respectively show the radiative and material temperature distributions obtained from the HLL and HLLC schemes. It is obvious that the HLL scheme induces an important numerical diffusion which affects the lower part of the domain. On the other hand, the HLLC scheme is able to deal properly with the discontinuity.

It appears in Table 1 that solution of the HLLC scheme with the asymptotic preserving correction and a second order MUSCL extension has a behavior very close to the exact solution.

Fig. 7 is a slice made at $x=1$m so that we can focus on the behavior of the radiative temperature across the contact discontinuity. We clearly see the effect of the numerical diffusion of the HLL scheme whereas the HLLC approximates quite closely the exact solution.

Table 1: Material temperature with HLL and HLLC schemes to compare with the exact solution given by $\|T\|_\infty = 1$ and $\|T\|_1 = 1$ (see Fig. 4).

Scheme	$\|T\|_\infty$		$\|T\|_1$	
	HLL	HLLC	HLL	HLLC
without AP	4300000	17000	350000	840
AP scheme	3600000	9000	43000	40
Minmod without AP	3600000	16000	240000	340
Minmod + AP	2700000	6400	34000	26
Superbee + AP	1600000	2400	11000	6.1

5.3 Venusian atmospheric entry

This last numerical application is devoted to the use of the HLLC scheme for radiative transfer in the framework of a full coupling between radiation and hydrodynamics. Indeed, in this numerical experiment, we look at the Venusian atmospheric entry of an object with the dimensions of the Pioneer Venus bus portion of the spacecraft that reached Venus in December 1978. The trajectory point considered in this simulation is located at an altitude of about 80km. At this point, the temperature is 142K and the pressure is 300Pa. Venusian atmospheric entries are known to be difficult because of the thickness of the atmosphere (about 90 times thicker than the Earth atmosphere). It has already been pointed out in [27] that the flow is modified by the radiative effects. Since a large amount of energy is dissipated thanks to radiative processes, a fully coupled model is required to predict the correct temperature profile.

The reader is referred to [11, 27] for details on the coupling between radiation and hydrodynamics. Here, we focus on the numerical accuracy improvements realized with use of the HLLC solver described earlier. Then for our study, we reduce the comparison to the HLL and HLLC approximate Riemann solvers at our disposal for the solution approximation of the radiative transfer equation. The calculation domain is regularly divided into 40 cells in the x direction and 15 cells in the y direction. The associated time step Δt is given by (2.21). The temperatures obtained with such flow conditions are plotted in Fig. 8. We can notice that the shock layer thickness is even more reduced through the use of the HLLC scheme than with the HLL scheme (compared to a non coupled simulation as shown in [27]).

Additionally, we refine the mesh in the boundary layer close to the body. This second mesh is still divided into 40 cells in the x direction and 15 cells in the y direction, as the original mesh, but is refined on the boundary of the probe. Fig. 9 shows the temperature predicted on the two different meshes by both HLL and HLLC schemes.

We can see that the HLLC scheme predicts similar results on both grids while the solution of the HLL scheme contains much more numerical diffusion on the first grid. We thus confirm the gain in accuracy we have made when developing an HLLC like Riemann solver. Moreover, from a computation cost point of view, performing these tests on one processor (type: Itanium II - 1.6 GHz), we outline that it is approximately two times longer to obtain a converged solution with the refined mesh than with the regular mesh. It is therefore cheaper to realize the needed calculations over a regular mesh, and it is accurate enough when using the HLLC approximate Riemann solver.

6 Conclusions

The present work concerns the derivation of an accurate scheme for the free streaming regime involved by the M_1 model for radiative transfer. During the last ten years, several numerical schemes have been proposed in the literature (for instance see [3, 5, 8, 9, 12, 15, 16]). These works essentially concern the difficult problem coming from the asymptotic preserving property. Indeed, one of the main property satisfied by the M_1
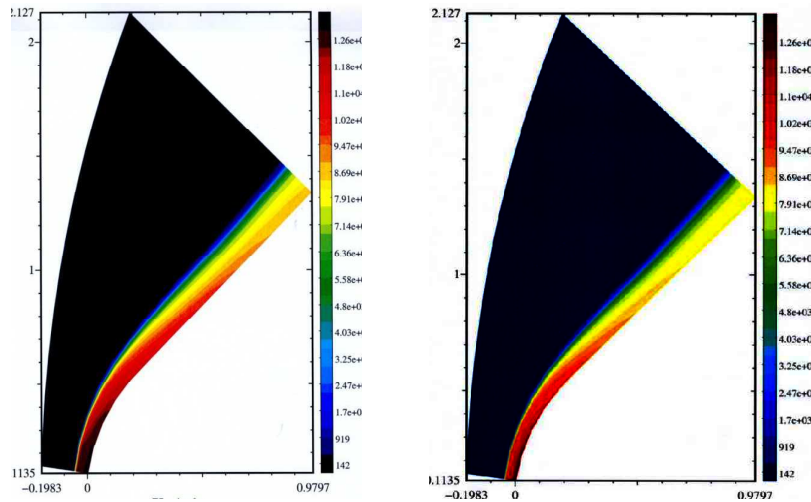
Figure 8: Temperatures obtained by the HLL (left) and HLLC (right) schemes.

model is its ability to restore the relevant diffusive limit.

Such a property turns out to be very difficult to be properly approximated by any numerical scheme. As a consequence, most of the suggested strategies consider an HLL (explicit or implicit) scheme for the transport part to obtain, with the suitable corrections, the required asymptotic preserving property.

We have here derived an HLLC-like scheme that is able to capture the stationary contact wave. Of course, such an accuracy property never holds involving a standard HLL method. In addition, this accurate method have been proved to be robust since it preserves the positiveness of the radiative energy and the required limitation of the radiative flux. Concerning the asymptotic diffusion regime of the scheme, we have adopted a recent Godunov-type scheme to include source terms as proposed in [6]. This approach is nothing but a suitable correction of the associated HLLC-like
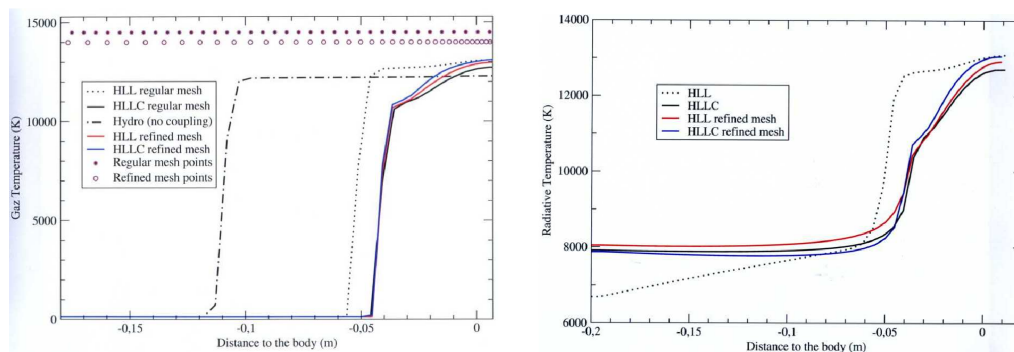

Figure 9: Gas temperature (left) and radiative temperature (right) - Mesh convergence.

Riemann solver. The use of this numerical technique ensures a judicious discretization of the source term and preserves a discrete limit diffusion equation. Several numerical experiments attest the relevance of the method and its ability to perform simulations of physical interest.

Appendix

The proof of the Theorem 2.1 easily comes from the next two statements. The first one is devoted to the equations satisfied by $\beta_x^\star$ and $\Pi^\star$.

Lemma A.1. *Assume U_L and U_R to be given in $\mathcal{A}$. The unknowns $\beta_x^\star$ and $\Pi^\star$ satisfy the relation* (2.17) *and* (2.18).

The second result concerns the existence of $\beta_x^\star$. Indeed, we have

Lemma A.2. *Assume U_L and U_R to be given in $\mathcal{A}$. The equation*

$$X^2 \tilde{F}_x^{HLL} - c\big(\tilde{P}_{xx}^{HLL} + E^{\star,HLL}\big)X + F_x^{\star,HLL} = 0,$$

admits two roots. One root remains in $(-1,1)$, while the second one is in $\mathbb{R}\backslash(-1,1)$.

Equipped with these two lemmas, we establish Theorem 2.1.

Proof. The existence and definition of $\beta_x^\star$ and $\Pi^\star$ easily come from Lemma A.1 and Lemma A.2.

Concerning the intermediate radiative energy $E_L^\star$ and $E_R^\star$, from (2.13), we have

$$\tilde{F}_{x,L} - F_{x,L} = -c(E_L^\star - E_L),$$
$$\tilde{F}_{x,R} - F_{x,R} = -c(E_R^\star - E_R).$$

Arguing about the linearization (2.15) associated with $\tilde{F}_{x,L,R}$, we immediately deduce the expected formulas (2.19a) and (2.19b). Since at this point $\beta_x^\star$ and $\Pi^\star$ are known, the radiative energies $E_L^\star$ and $E_R^\star$ are then fully defined.

The characterization of the other unknowns is a direct consequence of the linearization formulas (2.15) and the Rankine-Hugoniot relation (2.13) associated with F_y. The proof is thus completed. $\square$

To conclude the definition of the approximate Riemann solver, we prove the two technical lemmas.

Proof of Lemma A.1. From relation (2.13), we write

$$c(\tilde{P}_{xx,L} - P_{xx,L}) = -(F_{x,L}^\star - F_{x,L}), \tag{A.1}$$
$$c(\tilde{P}_{xx,R} - P_{xx,R}) = (F_{x,R}^\star - F_{x,R}). \tag{A.2}$$

The sum of these two relations gives

$$c(\tilde{P}_{xx,L} + \tilde{P}_{xx,R}) + (F_{x,L}^\star - F_{x,R}^\star) = 2c\tilde{P}_{xx}^{HLL},$$

where we substitute $\tilde{P}_{xx,L,R}$ and $F^\star_{x,L,R}$ with their associated linearization given by (2.15). We then obtain

$$\beta^\star_x(\tilde{F}_{x,L} + \tilde{F}_{x,R}) + 2c\Pi^\star + c\beta^\star_x(E^\star_L - E^\star_R) = 2c\tilde{P}_{xx,L}. \tag{A.3}$$

Once again, we use (2.13) to write

$$\tilde{F}_{x,L} + cE^\star_L = F_{x,L} + cE_L, \qquad \text{and} \qquad \tilde{F}_{x,R} - cE^\star_R = F_{x,R} - cE_R.$$

We plug these two relations into (A.3) to get

$$\beta^\star_x\big((F_{x,L} + cE_L) + (F_{x,R} - cE_R)\big) + 2c\Pi^\star = 2c\tilde{P}^{HLL}_{xx},$$

which rewrites in the expected form (2.18). Next, to establish (2.17), we first exhibit the following relation

$$F^{\star,HLL}_x = c\beta^\star_x(\Pi^\star + E^{\star,HLL}). \tag{A.4}$$

To access such an issue, we consider (A.1) and (A.2), where $F^\star_{x,L,R}$ and $\tilde{P}_{xx,L,R}$ are substituted with their corresponding linearization (2.15). We easily obtain

$$(\beta^\star_x)^2(E^\star_L + \Pi^\star) + \Pi^\star - P_{xx,L} = -\Big(\beta^\star_x(E^\star_L + \Pi^\star) - \frac{F_{x,L}}{c}\Big), \tag{A.5}$$

$$(\beta^\star_x)^2(E^\star_R + \Pi^\star) + \Pi^\star - P_{xx,R} = -\Big(\beta^\star_x(E^\star_R + \Pi^\star) - \frac{F_{x,R}}{c}\Big). \tag{A.6}$$

We introduce the relations (2.19a) and (2.19b) of $E^\star_{L,R}$ into (A.5) and (A.6) to write

$$(1 + \beta^\star_x)\Pi^\star + \beta^\star_x E_L - P_{xx,L} - (1 - \beta^\star_x)\frac{F_{x,L}}{c} = 0,$$

$$-(1 - \beta^\star_x)\Pi^\star + \beta^\star_x E_R - P_{xx,R} - (1 + \beta^\star_x)\frac{F_{x,R}}{c} = 0.$$

From the sum of these two above relations, we easily obtain the required relation (A.4). Next, the expected quadratic equation (2.17) satisfied by $\beta^\star_x$ is straightforwardly deduced from (2.18) and (A.4). The proof is achieved. $\qquad\square$

In order to prove Lemma A.2, we need the following technical result

Lemma A.3. *Assume U to be given in $\mathcal{A}$, then we have*

$$E + P_{xx} \pm 2F_x/c > 0.$$

Proof. After the work by Dubroca-Feugeas [12], the radiative energy E and the radiative flux F_x are the first two moments in the x-direction of a positive radiative intensity I. As a consequence, E and F_x rewrite as follows

$$E = <1, I>, \qquad \text{and} \qquad F_x/c = <\mu_x, I>,$$

where μ_x is the projection on the x-axis of the angular variable, and $< .,. >$ denotes a positive average operator. In addition, involving such notations, the radiative pressure is nothing but the following closure [12, 26]

$$P_{xx} = < \mu_x^2, I > .$$

Arguing such a reformulation, we have

$$E + P_{xx} \pm 2F_x/c = < (1 \pm \mu_x)^2, I >,$$

where by definition, $< (1 \pm \mu_x)^2, I >$ is positive. The proof is thus achieved.   □

Proof of Lemma A.2. Let us introduce the following auxiliary function

$$\Phi(X) = X^2 \tilde{F}_x^{HLL} - c(\tilde{P}_{xx}^{HLL} + E^{\star,HLL})X + F_x^{\star,HLL},$$

to study its roots. From (2.17), we know that $\beta_x^\star$ is one of these roots. Since Φ is a quadratic function, the result is established as soon as the product $\Phi(1)\Phi(-1)$ is proved to be negative. First, we write

$$\Phi(1) = \tilde{F}_x^{HLL} - c(\tilde{P}_{xx}^{HLL} + E^{\star,HLL}) + F_x^{\star,HLL}.$$

Involving the definition of $(\tilde{F}^{HLL}, \tilde{P}_{xx}^{HLL})$ and $(E^{\star,HLL}, F_x^{\star,HLL})$ given by (2.16a), we obtain after a straightforward computation

$$\Phi(1) = -c(E_R - 2F_{x,R}/c + P_{xx,R}).$$

Similarly, we have

$$\Phi(-1) = \tilde{F}_x^{HLL} + c(\tilde{P}_{xx}^{HLL} + E^{\star,HLL}) + F_x^{\star,HLL},$$

to obtain the following relation

$$\Phi(-1) = c(E_L - 2F_{x,L}/c + P_{xx,L}).$$

From Lemma A.3, we immediately obtain

$$\Phi(-1) > 0, \quad \text{and} \quad \Phi(1) < 0,$$

and the proof is achieved.   □

References

[1] R. ABGRALL, V. PERRIER, *Asymptotic expansion of a multiscale numerical scheme for compressible multiphase flow*, SIAM. Multiscale. Model. Simul., 5 (2006), pp. 84–115.
[2] P. BATTEN, N. CLARKE, C. LAMBERT, D.M. CAUSON, *On the choice of wavespeeds for the HLLC Riemann solver*, SIAM. J. Sci. Comput., 18 (1997), pp. 1553–1570.

[3] C. BERTHON, P. CHARRIER, B. DUBROCA, *An asymptotic preserving relaxation scheme for a moment model of radiative transfer*, C. R. Acad. Sci. Paris., Ser. I, 344 (2007), pp. 467–472.

[4] C. BERTHON, P. CHARRIER, B. DUBROCA, *An HLLC scheme to solve the M_1 model of radiative transfer in two space dimensions*, J. Scie. Comput., 31 (2007), pp. 347–389.

[5] C. BERTHON, J. DUBOIS, R. TURPAULT, *Numerical Approximation of the M_1 Model*, Editions SMF, Panoramas et synthèses 28 (2009).

[6] C. BERTHON, R. TURPAULT, *Asymptotic preserving HLL schemes*, Numer. Meth. Part. D. E., to appear.

[7] F. BOUCHUT, Nonlinear Stability of Finite Volume Methods for Hyperbolic Conservation Laws, and Well-Balanced Schemes for Sources, Frontiers in Mathematics series, Birkhauser, (2004).

[8] C. BUET, S. CORDIER, *An asymptotic preserving scheme for hydrodynamics radiative transfer models: numerics for radiative transfer*, Numer. Math., 108 (2007), pp. 199–221.

[9] C. BUET, B. DESPRÉS, *Asymptotic preserving and positive schemes for radiation hydrodynamics*, J. Comput. Phys., 215 (2006), pp. 717–740.

[10] C. BUET, B. DESPRÉS, *Asymptotic analysis of fluid models for the ocupling of radiation and hydrodynamics*, J. Quant. Spectrosc. Radiat. Transfer., 85 (2004), pp. 385–418.

[11] P. CHARRIER, B. DUBROCA, G. DUFFA, R. TURPAULT, *An implicit preconditionned JFNK method for fully coupled radiating flows, application to superorbital re-entry simulations*, Proceedings of Third Internationnal Conference on Computationnal Fluid Dynamics, (2004).

[12] B. DUBROCA, J.-L. FEUGEAS, *Hierarchie de modeles aux moments pour le transfert radiatif*, C. R. Acad. Sci. Paris, 329 (1999), pp. 915–920.

[13] C. A. J. FLETCHER, Computational Techniques for Fluid Dynamics - Specific Techniques for Different Flow Categories, Springer-Verlag, (1988).

[14] M. GONZALEZ, *Contribution à l'étude numérique de l'hydrodynamique radiative: des expériences de chocs radiatifs aux jets astrophysiques*, PhD Thesis, Université Paris-Sud XI, (2006).

[15] L. GOSSE, G. TOSCANI, *Asymptotic-preserving well-balanced scheme for the hyperbolic heat equations*, C. R. Acad. Sci. Paris, 334 (2002), pp. 337–342.

[16] T. GOUDON, Mathematical Models and Numerical Methods for Radiative Transfer, Editions SMF, Panoramas et synthèses, 28 (2009).

[17] A. HARTEN, P. D. LAX, B. VAN LEER, *On upstream differencing and godunov-type schemes for hyperbolic conservation laws*, SIAM. Rev., 25 (1983), pp. 35–61.

[18] J. C. HAYES, M. L. NORMAN, *Beyond flux-limited diffusion: parallel algorithms for multidimensional adiation hydrodynamics*, ApJS., 147 (2003), pp. 197–220.

[19] R. J. LEVEQUE, Finite Volume Methods for Hyperbolic Problems, Cambridge Texts in Applied Mathematics, (2002).

[20] D. LEVERMORE, *Relating eddington factors to flux limiters*, J. Quant. Spectrosc. Radiat. Transfer., 31 (1984), pp. 149–160.

[21] D. MIHALAS, G. W. MIHALAS, Foundation of Radiation Hydrodynamics, Oxford University Press, (1984).

[22] G. C. POMRANING, The Equations of Radiation Hydrodynamics, Sciences Application, (1973).

[23] S. RICHLING, E. MEINKÖHN, N. KRYZHEVOI AND G. KANSCHAT, *Radiative transfer with finite elements: I. basic method and tests*, Astron. Astrophys., 452 (2001), pp. 907–920 .

[24] E. F. TORO, Riemann Solvers and Numerical Methods for Fluid Dynamics - A Practical Introduction, Springer-Verlag Berlin Heidelberg, (1999).

[25] E. F. TORO, M. SPRUCE, W. SPEARE, *Restoration of the contact surface in the HLL Riemann*

solver, Shock. Waves., 4 (1994), pp. 25–34.

[26] R. TURPAULT, *A consistant multigroup model for radiative transfer and its underlying mean opacities*, J. Quant. Spectrosc. Radiat. Transfer., 94 (2005), pp. 357–371.

[27] R. TURPAULT, *Modélisation, Approximation Numérique et Applications du Transfert Radiatif en Déséquilibre Spectral Couplé avec L'hydrodynamique.*, PhD Thesis, Université Bordeaux 1, (2003).